

*Citation for published version:*

Bimbo, N, Zhang, K, Aggarwal, H, Mays, TJ, Jiang, J, Barbour, LJ & Ting, VP 2021, 'Hydrogen Adsorption in Metal-Organic Framework MIL-101(Cr) - Adsorbate Densities and Enthalpies from Sorption, Neutron Scattering, *in Situ* X-ray Diffraction, Calorimetry, and Molecular Simulations', *ACS Applied Energy Materials*, vol. 4, no. 8, pp. 7839-7847. <https://doi.org/10.1021/acsaem.1c01196>

*DOI:*

[10.1021/acsaem.1c01196](https://doi.org/10.1021/acsaem.1c01196)

*Publication date:*

2021

*Document Version*

Peer reviewed version

[Link to publication](#)

This document is the Accepted Manuscript version of a Published Work that appeared in final form in ACS Applied Energy Materials, copyright © 2021 American Chemical Society after peer review and technical editing by the publisher. To access the final edited and published work see <https://pubs.acs.org/doi/10.1021/acsaem.1c01196>

**University of Bath**

## **Alternative formats**

If you require this document in an alternative format, please contact:  
[openaccess@bath.ac.uk](mailto:openaccess@bath.ac.uk)

### **General rights**

Copyright and moral rights for the publications made accessible in the public portal are retained by the authors and/or other copyright owners and it is a condition of accessing publications that users recognise and abide by the legal requirements associated with these rights.

### **Take down policy**

If you believe that this document breaches copyright please contact us providing details, and we will remove access to the work immediately and investigate your claim.

**Final version, post review and revision.** Bimbo, N.; Aggarwal, H.; Zhang, K.; Mays, T. J.; Jiang, J.; Barbour, L. J.; Ting, V. P., Hydrogen adsorption in metal-organic framework MIL-101(Cr) - Adsorbate densities and enthalpies from sorption, neutron scattering, *in situ* X-ray diffraction, calorimetry, and molecular simulations. *ACS Applied Energy Materials* **2021**, *4*, 7839-7847. DOI: [10.1021/acsaem.1c01196](https://doi.org/10.1021/acsaem.1c01196).

## Hydrogen Adsorption in Metal-Organic Framework MIL-101(Cr) – Adsorbate Densities and Enthalpies from Sorption, Neutron Scattering, *In-Situ* X-ray Diffraction, Calorimetry, and Molecular Simulations

Nuno Bimbo<sup>1\*</sup>, Kang Zhang<sup>2,3</sup>, Himanshu Aggarwal<sup>4\*</sup>, Timothy J. Mays<sup>5</sup>, Jianwen Jiang<sup>2</sup>, Leonard J. Barbour<sup>4</sup>, Valeska P. Ting<sup>6\*</sup>

<sup>1</sup>School of Chemistry, Highfield Campus, University of Southampton, Southampton, SO17 1BJ, United Kingdom

<sup>2</sup>Department of Chemical and Biomolecular Engineering, National University of Singapore, 117576, Singapore

<sup>3</sup>Institute of Advanced Materials and Flexible Electronics (IAMFE), School of Chemistry and Materials Science, Nanjing University of Information Science & Technology, 210044, Nanjing, China

<sup>4</sup>Department of Chemistry and Polymer Science, University of Stellenbosch, Matieland 7600, South Africa

<sup>5</sup>Department of Chemical Engineering, University of Bath, Claverton Down, Bath, BA2 7AY, United Kingdom

<sup>6</sup>Department of Mechanical Engineering, University of Bristol, Bristol BS8 1TR, United Kingdom

\*Corresponding authors:

Dr Nuno Bimbo

School of Chemistry, Highfield Campus, University of Southampton, Southampton, SO17 1BJ, United Kingdom

E-mail: [n.bimbo@soton.ac.uk](mailto:n.bimbo@soton.ac.uk)

Prof Valeska P Ting

Department of Mechanical Engineering, University of Bristol, Bristol BS8 1TR, United Kingdom

E-mail: [v.ting@bristol.ac.uk](mailto:v.ting@bristol.ac.uk)

\*Current address: Department of Chemistry, Birla Institute of Technology & Science (BITS), Pilani, Hyderabad Campus, Hyderabad, 500078 Telangana, India

**Keywords:** Hydrogen storage; metal-organic frameworks; MIL-101(Cr); inelastic neutron scattering; enthalpies of adsorption; adsorbed density.

### Abstract

In this paper, hydrogen adsorption in metal-organic framework (MOF) MIL-101(Cr) is investigated through a combination of sorption experiments, modelling of experimental isotherms, differential scanning calorimetry, neutron scattering, *in-situ* synchrotron powder X-ray diffraction, and molecular simulations. The molecular simulations at 77 K for H<sub>2</sub> adsorption in the material show excellent correspondence with excess uptakes determined from experimental isotherms. The simulations also indicate that H<sub>2</sub> adsorption at a low pressure is mainly located in the 0.7 nm super-tetrahedron and then with increasing pressure H<sub>2</sub> starts to accumulate in the small (2.9 nm) and large (3.4 nm) cages with increasing pressure. The inelastic neutron scattering results show that, in contrast to reports for hydrogen adsorption under the same conditions for microporous carbons, there is no solid-like H<sub>2</sub> or any higher density H<sub>2</sub> phases adsorbed in the pores of MIL-

101(Cr). This indicates that, with increasing pressures, the adsorbed density of the MIL-101(Cr) remains constant but the volume of adsorbate increases, and that higher densities for adsorbed hydrogen require pore sizes smaller than 0.7 nm, which is the size of the smallest pore in MIL-101(Cr). The enthalpies of adsorption are also investigated for this material using simulations, the Clapeyron equation applied to the isosteres and differential scanning calorimetry, with the direct calorimetric method showing good agreement at zero-coverage with the other two methods. The simulations and the Clapeyron equation are also in good agreement up to 6 wt.% coverage.

## Introduction

As a low-carbon, non-polluting alternative to fossil fuels, the widespread utility of green molecular hydrogen (H<sub>2</sub>) as a sustainable energy vector for mobile applications is inhibited by the difficulties associated with storing it at acceptably high densities for practical applications [1, 2]. Gaseous H<sub>2</sub> above its bulk liquid-vapour critical temperature of 33 K will not condense to form a higher-density bulk liquid or a solid with increasing pressure making the efficient and economic storage of molecular H<sub>2</sub> a major technological challenge [1]. One option for increasing storage densities is via adsorption of H<sub>2</sub> in microporous materials, i.e., materials with pore diameters below 2 nm, as micropore volume has shown to be well-correlated with higher H<sub>2</sub> uptakes [3]. In these materials, densification of H<sub>2</sub> is promoted via the enhancement of attractive van der Waals interactions between the adsorbed H<sub>2</sub> molecules and the solid substrate, arising from overlapping potentials from opposite pore walls. With many porous materials being developed as potential storage media, especially high-surface area adsorbents such as metal-organic frameworks (MOFs), the ability to quickly and accurately screen materials for their gas storage properties is a valuable tool for accelerating progress in this area, as has been shown recently in a number of studies [4, 5].

Hydrogen storage materials have been fully characterised over the past decade and a number of helpful metrics have been used to assess these. The US Department of Energy has put forward system storage targets for onboard light-duty vehicles, which include gravimetric and volumetric capacities, delivery pressures and temperatures, cost, charging and discharging times, and fuel purity [6]. Looking specifically at porous materials, there are many helpful parameters that have been developed to assess materials. Hydrogen storage capacities at 77 K correlate very well with the Brunauer-Emmett-Teller (BET) surface area [7]. This was developed into an empirical rule that has become known as Chahine's rule, which states that there will be approximately 1 wt.% H<sub>2</sub> uptake at 77 K and 2 MPa for every 500 m<sup>2</sup> g<sup>-1</sup> of measured BET surface area in the material

[3, 7, 8]. More recently, Noguera-Díaz et al. showed similar types of correlations, using BET surface areas and por volumes to determine total hydrogen uptakes in a range of MOFs [9]. Equally important for H<sub>2</sub> storage is the pore size of the adsorbent material, and it has been argued that ultramicropores (widths below 0.7 nm) are thought to contribute the most to storage of hydrogen in a porous material [10-13]. More recently, other parameters such as void fraction and volumetric surface area have been used to guide large scale screening of potential H<sub>2</sub> storage materials [4]. Using these large scale screening methods, MOF NU-1501-Al was reported with one of the largest reported surface areas (7,310 m<sup>2</sup> g<sup>-1</sup>) alongside exceptional methane and H<sub>2</sub> uptake [5].

One important aspect to consider for H<sub>2</sub> storage in porous materials is the adsorbed density. It has been shown, through a combination of modelling and inelastic neutron scattering, that hydrogen can be highly densified in the pores of an activated carbon [14]. That work showed how H<sub>2</sub> could reach solid-like densities in these structures, with density values that surpassed 100 kg m<sup>-3</sup> (solid parahydrogen at 4 K and 1.2 MPa has a density of 87.6 kg m<sup>-3</sup> [15]). More recently, a follow-up study showed the same type of densification in two other carbons, a titanium carbide-derived carbon and a single-walled carbon nanotube [16]. Understanding densification processes in H<sub>2</sub> storage materials is a critical aspect when investigating adsorbent storage. Whereas available surface area seems to correlate well with uptake of H<sub>2</sub>, the densification that occurs upon adsorption is still not very well understood, and any insights into structure or morphology of the material that contributes to higher density states would guide the synthesis of new materials. These insights would be especially important for materials such as MOFs, which have very high BET surface areas and tuneable pore sizes and chemistry.

In addition to densities, design of complete H<sub>2</sub>-based energy systems also requires knowledge of the fundamental thermodynamic variables for the system. The isosteric enthalpies of adsorption are an indication of the strength of the adsorption interaction. Higher enthalpies indicate stronger interactions between the H<sub>2</sub> and the adsorbent, allowing for some hydrogen to be adsorbed at close to ambient temperatures for enthalpies >15 kJ mol<sup>-1</sup>. Conversely, if the enthalpies are too high (i.e. above 50 kJ mol<sup>-1</sup>, as in the case of chemisorption), problems arise with removal of the hydrogen from the storage medium. As storage capacities are heavily dependent on the temperature of storage, accurate values for isosteric enthalpies are needed for calculation of the heat released during the exothermic adsorption step so that appropriate heat management

systems can be put in place. Hydrogen typically has low energies of interaction, which are reflected in the low enthalpies of adsorption, which is why significant uptakes are only obtained at cryogenic temperatures. There are also issues with correctly assessing enthalpies of adsorption. Experimental approaches to measuring enthalpies include calorimetric methods (which rely on detection of the heat released during adsorption) and techniques such as temperature programmed desorption (which use changes in pressure or mass spectrometry to track the desorption of adsorbed molecules as a function of increasing temperature [17-20]). However, these experiments are generally only performed on systems involving chemisorption of hydrogen, where the enthalpy changes involved ( $> 50 \text{ kJ mol}^{-1}$ ) are higher than for physisorption (ca.  $5\text{-}10 \text{ kJ mol}^{-1}$ ). Therefore, indirect methods of determining the enthalpies of  $\text{H}_2$  sorption would be preferable if the enthalpies resulting from such calculations prove reliable. As calorimetry has been especially hard to reconcile with other methods, the most common method for estimating enthalpies of adsorption for  $\text{H}_2$  in porous materials has been through the isosteric method. This requires measurement of the adsorption excess isotherms at different temperatures, which are then evaluated using different methods (usually the Clausius-Clapeyron approximation or the virial equation) in order to obtain estimates of the enthalpies of adsorption [21, 22].

In addition to experimental methods, computational modelling and simulation have proven a very valuable tool to reduce the time and effort in screening potential materials and predict gas uptakes for a variety of systems. Molecular simulation allows prediction of the behaviour of a material and its properties under conditions of pressure and temperature which cannot easily be attained experimentally [23]. In addition, simulation can be used to look more closely at the origins of such phenomena as density distributions and enthalpies of adsorption from a molecular viewpoint, providing insights into supercritical adsorptive storage at a molecular level [23]. Furthermore, simulation does not rely on the production of a pure-phase product, and can even be performed on theoretical materials or those that are challenging to synthesise. However, complex materials can be computationally expensive to model and new or unusual results are sometimes treated with scepticism. Molecular modelling has been especially useful to look at new materials such as MOFs [23]. MOFs are one of the newest classes of designer porous materials and have been tested for many applications in gas storage and separations, but many MOFs have very complex structures, and thus can be difficult to accurately describe with molecular modelling techniques. Due to the large number of MOF materials that could potentially be investigated for gas storage,

it is essential that methods designed to evaluate and screen these materials for capacities (i.e. isotherm models and molecular modelling) give consistent and accurate results.

In order to further study hydrogen densification processes that occur in porous materials, and to gain some insight into the enthalpies associated with hydrogen adsorption, we have looked at a well-studied MOF (MIL-101(Cr)) and studied its hydrogen adsorption with a range of experimental and modelling tools. MIL-101(Cr) is an exceptionally stable MOF with very high-surface area ( $\sim 4,100 \text{ m}^2 \text{ g}^{-1}$ ), and a very high capacity for  $\text{H}_2$  storage [24, 25]. It was first described as a “giant pore” MOF, and the *Fd3hm* unit cell is appropriately large, with unit dimensions of  $\sim 8.9 \text{ nm}$ , and an exceptionally large cell volume ( $702 \text{ nm}^3$ ). The structural features of MIL-101(Cr) also make it a challenging structure to model, due to the existence of three distinct pore sizes:  $0.7 \text{ nm}$  (supertetrahedra),  $2.9 \text{ nm}$  and  $3.4 \text{ nm}$  [26]. MIL-101(Cr) has been widely studied in the literature for hydrogen adsorption. The material is an excellent example model material for the investigation of the densification processes occurring in hydrogen adsorption, as it is a metal-organic framework with high-surface area, excellent hydrogen uptake, an exceptional pore volume and three different pore sizes, covering both the micro and mesopore range. The surface heterogeneity provided by the unsaturated Cr metal centres also makes estimates of the isosteric enthalpies of adsorption more difficult than would be the case for a material with a more chemically homogeneous adsorbing surface. In order to be able to understand the densification phenomena, we use a combination of *in-situ* synchrotron X-ray diffraction, to assess any changes in the structure, and inelastic neutron scattering, to evaluate the density of the adsorbed  $\text{H}_2$ . This is complemented with previous modelling results obtained on the experimental isotherms and molecular simulations on the material. The enthalpies of adsorption are also studied for the material, with a combination of methods that includes the Clapeyron equation applied using the isosteric method, molecular simulations and differential scanning calorimetry.

## Results and Discussion

Molecular simulations and methodologies that analyse excess isotherms to determine absolute and total uptakes in porous solids are usually predicated on the assumption that the pore volume (the adsorption space) is constant. In previous reports, a model was presented that distinguishes between total, absolute and excess adsorption to analyse experimental isotherms [27-29], and the constant volume for adsorption was assumed to be the pore volume. The pore volume in the

modelling can either be the result of fitting the model to experimental data, (a parameter results from the fitting based on the best value for the pore volume that fits the experimental data), or it can be used as a fixed parameter. If the latter, then a value needs to be provided, which is usually the experimentally determined value for the pore volume, determined from the application of a given method (Dubinin-Radushkevich, Barrett-Joyner-Halenda, DFT or others) to the nitrogen isotherm at 77 K [22]. This can cause some uncertainties, as the molecular dimensions are different (nitrogen has a kinetic diameter of 0.364 nm and hydrogen has a kinetic diameter of 0.289 nm), so the accessible pore volume to the different probe molecules is different.

Molecular simulations also assume constant volume of MIL-101(Cr) for adsorption. Verifying the constant volume assumption is important for MOFs, as many of these structures have been reported to be flexible [30]. The flexibility in these structures has been reported to be induced mechanically, chemically, through light, or other stimuli [31]. In order to investigate the flexibility of the structure under different conditions and to ensure the validity of assumptions in the modelling and computer simulations (constant pore volume), the unit cell of MIL-101(Cr) was investigated using synchrotron powder X-ray diffraction at the European Synchrotron Radiation Facility (ESRF) in Grenoble, in a sample cell that was equipped for *in-situ* gas dosing (details in Supporting Information). The temperatures ranged from 80 to 300 K and the pressure ranged from 0 up to 10 MPa. In order to benchmark those changes, we also tested a material known for its flexibility, MOF MIL-53(Al) [32], under the same conditions, and have presented those results in Supporting Information. The results for the synchrotron powder X-ray diffraction carried out at 0 and 10 MPa and 100 and 300 K are shown in Figure 1. As it can be observed, the material is quite stable at different conditions, with the unit cell of MIL-101(Cr) showing no pressure dependence, and only minimal temperature dependence at cryogenic conditions. This is in contrast to MIL-53(Al) (Fig.S1 in Supporting Information), which shows both pressure and temperature dependence of the unit cell under the same conditions.

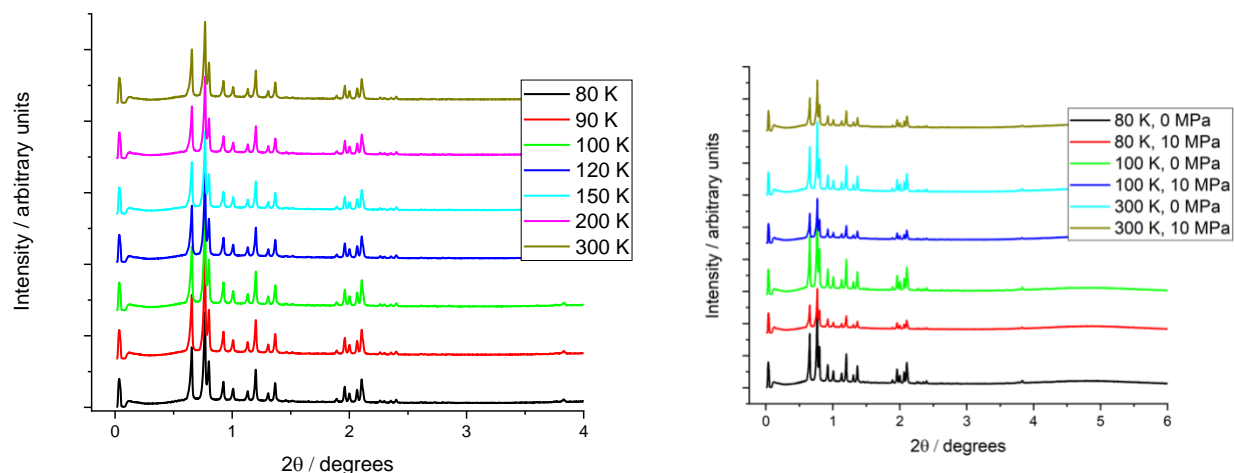


**Figure 1 – *In-situ* synchrotron powder X-ray diffraction spectra of MIL-101(Cr). Left – low-angle diffraction spectra measured from 80 to 300 K. Right – low-angle diffraction spectra measured at 80, 100 and 300 K at 0 and 10 MPa of hydrogen pressure.**

The next stage was to evaluate the hydrogen uptakes in these structures using a combination of experiments and computer simulations to gain some insights into in-pore densification processes. Hydrogen isotherms at a range of temperatures for MIL-101(Cr) (isotherms at some of the temperatures were previously reported [27, 28]) were measured from 77 K to room temperature and up to 12 MPa (see Fig 2A). The data in Figure 2, acquired from 77 to 292 K and from 0 to 12 MPa, is in the range expected and reported in other papers for hydrogen adsorption in MIL-101 (Cr) [24, 33, 34]. In order to use computer simulations as an indication of the processes that occur during hydrogen adsorption, the first step was to compare amounts adsorbed using computational simulation and modelling applied to experimental gas uptake results.

The details for the simulation methodology are provided in the Supporting Information. We have adopted Gibbs Ensemble Monte Carlo (GEMC) method, which allows the direct calculation of the excess isotherm. The pressure is an input in the GEMC method, as demonstrated in a previous study [35]. Specifically, two simulation boxes (one for the adsorbent and the other for the bulk adsorbate) are used and allow adsorbate molecules to change between the two boxes. From GEMC method, the bulk density, enthalpy, and excess amounts can be easily calculated (more details in Supporting Information). We find excellent correspondence in Fig. 2B between the simulated excess uptakes and experimentally obtained values. As the uptakes between the model and the simulations were in good correspondence, the simulation snapshots are provided in order to gain microscopic insight into the adsorption and densification process that occurs for hydrogen in MIL-101(Cr). As seen in Fig S2 in Supporting Information, at a low pressure, H<sub>2</sub> is located in the super-tetrahedron; with increasing pressure, H<sub>2</sub> starts to locate in the small and large cages.



In Fig 2B, the total and absolute hydrogen uptake are also shown for the MIL-101(Cr). These were calculated using a methodology that was previously reported [29, 36] that distinguishes between excess, absolute and total adsorption, assuming a constant density of adsorbate and available pore volume. The excess is the amount of adsorbed hydrogen determined experimentally, absolute refers to the amount in the pore with a higher density than the bulk (the density is assumed constant, with the volume of adsorbate increasing with pressure) and the total refers to the total amount of gas within the pore (that is, the absolute, which is the denser phase, and the bulk gas present in the pore). Excess, absolute and total adsorption are represented in Eqs. 1, 2 and 3, respectively.

$$m_e = \rho_a \theta V_p - \rho_b \theta V_p \leftrightarrow (\rho_a - \rho_b) \theta V_p \quad (\text{Eq.1})$$

$$m_a = m_e + \rho_b \theta V_p \leftrightarrow \rho_a \theta V_p \quad (\text{Eq.2})$$

$$m_t = m_e + \rho_b V_p \leftrightarrow \rho_a \theta V_p + \rho_b V_p (1 - \theta) \quad (\text{Eq.3})$$

In Eqs.1, 2 and 3,  $m_e$  is excess adsorption,  $m_a$  is absolute adsorption,  $m_t$  is total adsorption,  $\rho_a$  is the density of the adsorbed phase,  $\rho_b$  is the density of the bulk phase,  $\theta$  is the fractional filling of the micropore, and  $V_p$  is the pore volume. The uptakes are reported in wt.%, which is mass of hydrogen over mass of degassed sample, the density units for  $\rho_a$  and  $\rho_b$  are  $\text{kg m}^{-3}$ , the filling function  $\theta$  is dimensionless and  $V_p$  is in units of  $\text{cm}^3 \text{g}^{-1}$  (g refers to the mass of adsorbent material). The fractional filling  $\theta$  can be represented using any type I equation. The Tóth equation [37, 38] (Eq.4) is known to produce good results to fitting experimental data under these conditions [29].

$$\theta = \frac{bP}{[1+(bP)^c]^{1/c}} \quad (\text{Eq. 4})$$

In the fittings previously reported [29, 36],  $\rho_b$  is determined from a rational function fitted to the NIST data, which is based on the Leachman's equation of state for normal hydrogen [36, 39]. The temperature dependence of fitting similar models to hydrogen adsorption in metal-organic frameworks, including MIL-101(Cr), has been investigated in the past [29] and parameters such as the adsorbed phase density were shown not to display an obvious temperature dependence. For this reason and as done in previous studies [14, 27, 36], the adsorbed phase density and the

pore volume were assumed constant for all temperatures. The Tóth heterogeneity parameter and the Tóth  $b$  parameter were only fitted to the adsorption data at 77 K. This means that the parameters  $b$ ,  $c$ ,  $V_p$  and  $\rho_a$  are determined from the fittings, with  $V_p$  and  $\rho_a$  constant for all of the temperatures that were fitted (77, 90, 100 and 110 K) and  $b$  and  $c$  specific for each temperature. The results from the fitting are presented in Table 1. The micropore volume, which is a parameter determined from the fit, has a value of  $1.6 \text{ cm}^3 \text{ g}^{-1}$ . This is a value that is very close to the pore volumes for the same material obtained using nitrogen and hydrogen adsorption and the Gurvich rule by Streppel and Hirscher [26], which were 1.51 and  $1.50 \text{ cm}^3 \text{ g}^{-1}$ , respectively.

**Table 1 – Fitting parameters for the multifit to hydrogen isotherms on MIL-101(Cr) at 77, 90, 100 and 110 K. The  $\pm$  uncertainty refers to the standard error from the nonlinear fitting. Table adapted and reproduced with permission from reference [29]. Copyright 2013 Springer.**

	MIL-101(Cr)
Adsorbate density, $\rho_a / \text{kg m}^{-3}$	$72.4 \pm 3.5$
Micropore volume, $V_p / \text{cm}^3 \text{ g}^{-1}$	$1.6 \pm 0.5$
Tóth $b$ parameter at 77 K / $\text{MPa}^{-1}$	$6.0 \pm 2.8$
Tóth heterogeneity parameter at 77 K, $c / -$	$0.36 \pm 0.09$

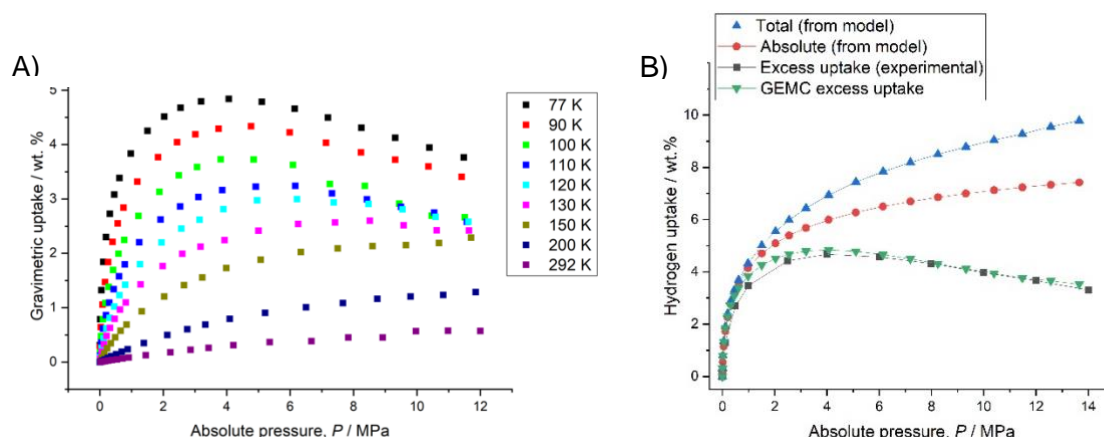


**Figure 2 – A) Hydrogen isotherms from 77 to RT, with data adapted and reproduced with permission from reference [27]. Copyright 2013 Springer. B) Comparison between GEMC simulated amounts and the excess, and the absolute and total uptakes determined from the experimental excess.**

In order to probe the densification of hydrogen and investigate the presence of a high density, solid-like phase in MIL-101(Cr), we applied the same methodologies used in the past to analyse denser phases of hydrogen in microporous carbon TE7, titanium carbide-derived carbon and single-walled carbon nanotubes [14, 16]. Inelastic neutron scattering (INS) is a very powerful

**Final version, post review and revision.** Bimbo, N.; Aggarwal, H.; Zhang, K.; Mays, T. J.; Jiang, J.; Barbour, L. J.; Ting, V. P., Hydrogen adsorption in metal-organic framework MIL-101(Cr) - Adsorbate densities and enthalpies from sorption, neutron scattering, *in situ* X-ray diffraction, calorimetry, and molecular simulations. *ACS Applied Energy Materials* **2021**, *4*, 7839-7847. DOI: [10.1021/acsaem.1c01196](https://doi.org/10.1021/acsaem.1c01196).

technique that provides information about the adsorbed phase of hydrogen that is not possible to obtain using other techniques. Neutrons can penetrate deeply into solid matter and, unlike X-rays, are highly sensitive to the presence of hydrogen. Also, unlike infrared or Raman scattering, the molecular motion (vibration or rotation) detected by neutrons is not dependent on selection rules. INS can therefore provide extra information on the state and strength of the interactions of molecular hydrogen on MIL-101(Cr) at cryogenic temperatures and high pressures, allowing to probe the density of the adsorbed phase. INS was used to show the first experimental evidence of solid-like hydrogen at 77 K in the pores of an activated carbon (TE7). This was further complemented with modelling done on the experimental excess isotherms, which showed densities of adsorbed hydrogen in excess of  $100 \text{ kg m}^{-3}$ . More recently, INS and computational simulations were used to study three different carbons – TE7, single-walled carbon nanotubes and a titanium carbide-derived carbon – and again showed how pore sizes in the range of 0.7 nm led to significant hydrogen densification and the presence of a solid-like hydrogen phase [16]. In order to verify if the same phenomena were happening in the MIL-101(Cr), we carried out inelastic neutron scattering experiments in the same instrument used in both studies (TOSCA at the ISIS neutron source at the STFC Rutherford Appleton Laboratory, UK) at 77 K under increasing pressures of hydrogen (0 to 3 MPa). As noted in Table 1, the adsorbed hydrogen density for the MIL-101(Cr) determined from modelling of experimental isotherms was  $72.4 \text{ kg m}^{-3}$  (c.f. adsorbed densities of  $101.3 \text{ kg m}^{-3}$  for TE7 carbon using the same methodology). In order to check for the presence of solid hydrogen in the MIL-101(Cr) material, we used inelastic neutron scattering on the MIL-101(Cr) under increasing pressures of hydrogen, with results shown in Fig.3.

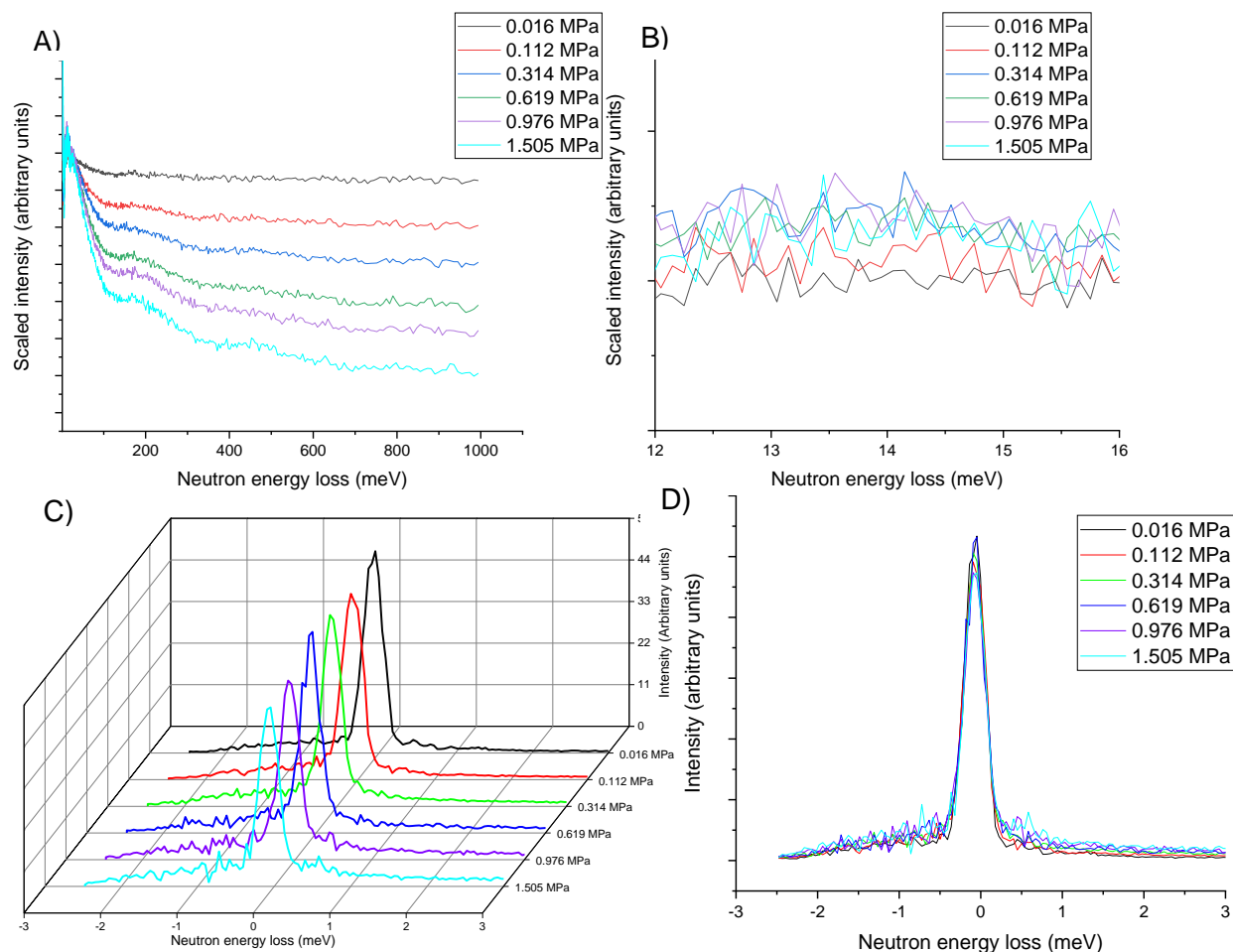


**Figure 3 – Inelastic neutron scattering (INS) done on the MIL-101(Cr) for increasing hydrogen pressures (from 0.016 to 1.505 MPa). A) INS with scaled intensities for different pressures. B) The rotor peak region for solid hydrogen (14.7 meV). C) The elastic line (-3 to 3 meV) with the Z-axis as the pressures. D) The elastic line (-3 to 3 meV) with the pressures superimposed.**

In Figure 3A and 3B, there is no clear rotor line at 14.7 meV, which was used previously to indicate the presence of solid-like hydrogen. The presence of the peak at 14.7 meV is taken as a fingerprint for solid hydrogen [40, 41]. The fact that no peak is observed for the MIL-101(Cr) at any pressure indicates that there is no solid-like hydrogen forming in the pores of MIL-101(Cr) at the conditions of the experiment (77 K and pressures up to 3 MPa). In addition to the lack of the 14.7 meV peak, there is also no change in the elastic line with increased pressure (Fig 3C and 3D), which also indicates that there are no higher density phases that approach liquid or solid-like hydrogen.

This, together with the results from the modelling of the experimental isotherms that show lower adsorbed hydrogen densities, indicate that a different mechanism for hydrogen densification to the one seen in the microporous carbons must be taking place here, or at least an adsorbed

phase density that is not as highly densified as the ones in the carbon studies. It should be important to note the differences between the TE7 and the MIL-101(Cr). The TE7 has a narrow pore size distribution and a chemically homogenous carbon surface with a slit pore geometry [14, 42]. The MIL-101(Cr) has a trimodal pore size (0.7, 2.9 and 3.4 nm) and a chemical heterogeneous surface [24]. Different explanations could be provided for the differences seen in hydrogen densification, including the heterogeneity of the adsorption sites of the MIL-101(Cr), or a non-ideal pore size or shape for hydrogen adsorption. For carbons, it has been shown that a pore size of 0.7 nm, which is the size of the small cage in the MIL-101(Cr), would result in very high densities of adsorbed hydrogen ( $\sim 120 \text{ kg m}^{-3}$ ) at 10 MPa, even at 300 K [43]. The inelastic neutron scattering results, together with the empirical modelling and the computer simulations, all indicate that there is no significant formation of a solid-like hydrogen density in the MIL-101(Cr) at these temperatures and pressures. It is interesting to note that, despite having higher hydrogen uptakes than the TE7 at most conditions of pressure and temperature, these results indicate that the density of the adsorbed hydrogen is smaller for the MIL-101(Cr). The fact that the elastic line retains the same full width at half maximum (FWHM) at different pressures and that this approaches the instrument's resolution ( $\sim 0.3 \text{ meV}$ ) suggests an insignificant proportion of the adsorbed hydrogen in a higher density hydrogen phase with increasing pressures [14]. What we postulate happens for the MIL-101(Cr) is that the hydrogen is adsorbed at higher densities in the pores of MIL-101(Cr), probably at densities close to what our modelling suggests ( $\sim 72 \text{ kg m}^{-3}$ ) as there is no solid-like hydrogen rotor peak or change in the elastic line. With increasing pressures and increasing amounts adsorbed, the density of adsorbed hydrogen remains stable (as the FWHM of the elastic line remains unaltered with increasing pressure), but the volume of adsorbed hydrogen increases in the pore. The results also show that there is an optimum pore size for higher adsorbed hydrogen densities, as the smallest pores in MIL-101(Cr) are 0.7 nm, and there is no solid-like formation, which suggests that smaller pores are needed for higher density phases. As suggested in the literature [10-12], it seems that pores in the ultramicroporous range ( $< 0.7 \text{ nm}$ ) are the ones contributing the most to the higher density phases of adsorbed hydrogen.

Along with adsorbed density, the enthalpy of adsorption is an important factor when evaluating  $\text{H}_2$  storage materials. However, determining these appropriately can be challenging, as noted in the introduction. There are different methods to estimate enthalpies of adsorption, including calorimetry, temperature programmed desorption or the isosteric method. The isosteric method relies on adsorption isotherms measured at different temperatures, which are then evaluated at

constant amounts adsorbed by applying the Clausius-Clapeyron equation. The Clausius-Clapeyron equation is derived from the exact thermodynamic equation for phase changes, which is the Clapeyron equation (Eq.5):

$$\left(\frac{dP}{dT}\right)_{n_a} = \frac{\Delta S}{\Delta v} \quad (\text{Eq.5})$$

The Clapeyron equation applies to any phase equilibria of any pure substance and it is commonly used for phase transitions occurring at vapour-liquid or solid-liquid boundaries. It relates the differential of pressure  $P$  with temperature  $T$  at constant amount adsorbed  $n_a$  (an isostere) to changes in entropy  $S$  and molar volume  $v$ . The entropy can be determined from the Second Law of Thermodynamics with the enthalpy  $H$  and temperature  $T$ , so Eq. 5 can be modified to yield the enthalpy of adsorption  $\Delta H_{\text{ads}}$ :

$$\left(\frac{dP}{dT}\right)_{n_a} = \frac{\Delta H_{\text{ads}}}{T\Delta v} \quad (\text{Eq.6})$$

The difficulty in determining both the differential for the isosteres over temperature at constant amount adsorbed, and the adsorbed molar volume, means that rather than using the Clapeyron equation, the Clausius-Clapeyron is the equation that is typically used for enthalpy calculations in adsorption. The phase transition referred to is the one that occurs between a molecule in the bulk and a molecule in the adsorbed phase and it relies on two main approximations, which are the negligible adsorbed molar volume when compared with the bulk molar volume ( $\Delta v$  becomes  $v_{\text{bulk}}$ ) and the ideal gas approximation (the molar volume of the bulk is calculated using the ideal gas equation). When these two approximations are applied to Eq.6, it becomes Eq.7:

$$\left(\frac{dP}{dT}\right)_{n_a} = \frac{\Delta H_{\text{ads}}P}{RT^2} \quad (\text{Eq.7})$$

in which  $R$  is the molar gas constant ( $8.314 \text{ J mol}^{-1} \text{ K}^{-1}$ ). A common way to present the Clausius-Clapeyron equation is in its integrated form (which assumes  $\Delta H_{\text{ads}}$ , is temperature independent) as shown in Eq.8

$$\ln P = \frac{\Delta H_{ads}}{R} \left( \frac{1}{T_i} - \frac{1}{T_f} \right) \quad (\text{Eq.8})$$

In Eq.8,  $T_i$  and  $T_f$  are the initial and final temperatures, respectively, and correspond to the temperatures at which the isotherms are measured. The isosteric enthalpies have been calculated for hydrogen at high pressures for the MIL-101(Cr) and the AX-21 activated carbon using the Clapeyron, the Clausius-Clapeyron and the virial equation, with the study concluding that there can be differences when using the different methods [27], indicating that the approximations of the Clausius-Clapeyron might not be valid for hydrogen adsorption at high pressures.

The use of the Clausius-Clapeyron equation means that isosteric enthalpies are usually represented as the as a function of coverage, as their determination relies on plotting the logarithm of the isostere (that is, the pressure at equal amount adsorbed) against the inverse temperatures. This can be calculated from just two temperatures, as seen in Eq.8. using a linear fit to the inverse temperatures. When using two or more temperatures, the enthalpy of adsorption for that amount adsorbed is the gradient of the linear fit through the inverse temperature. One of the consequences of this treatment is that the isosteric enthalpies are then solely a function of the coverage and are independent of temperature using this method. If instead the Clapeyron equation is applied to isotherm data (Eq.6), it can yield isosteric enthalpies at different temperatures as a function of coverage. In order to be able to do this, the isosteres need to be differentiated individually against temperature at constant amount adsorbed, and the adsorbed molar volumes need to be determined. As shown previously [27], both these can be achieved using a model that is applied to experimental data and can calculate absolute and total amounts adsorbed in the pore, making it more accessible to calculate isosteres and differences in molar volumes.

In order to compare adsorption enthalpies in the MIL-101(Cr) with direct measurement methods, we used high-pressure Differential Scanning Calorimetry (DSC), using a Setaram  $\mu$ DSC7 Evo module equipped with high-pressure sample holder coupled to a Setaram Hy-Energy PCTPro-2000. Details of the DSC experiments are in Supporting Information. As can be seen in Fig. 4A, the DSC showed an exothermic peak in the heat flow associated with adsorption at each dose pressure. The heat flows and hydrogen pressures are represented in Figure 4A, with the peak heights associated with the exothermic heat flow decreased with increasing dose pressure, as would be expected.

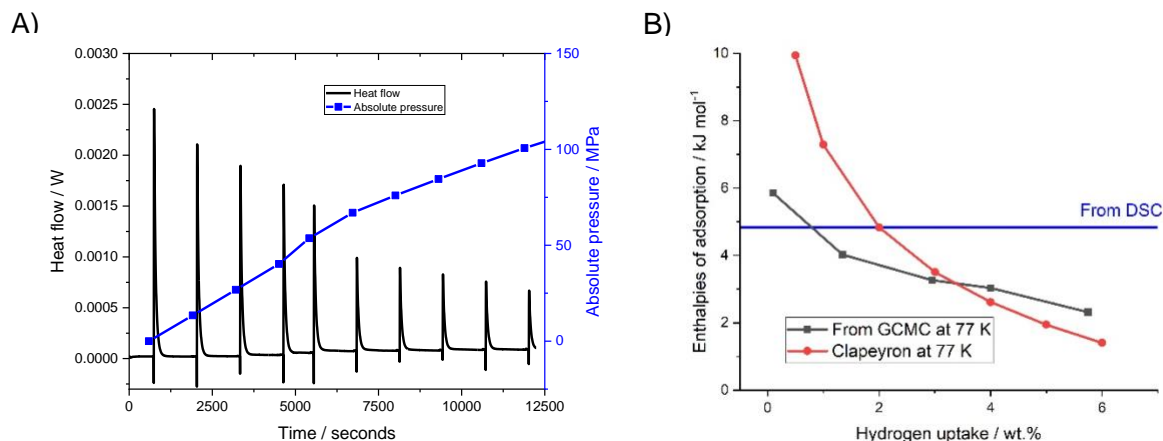


**Figure 4 – A) Differential Scanning Calorimetry carried out at 300 K using a high-pressure calorimeter coupled to a high-pressure volumetric apparatus. B) The calorimetric enthalpies and the enthalpies of adsorption calculated from GEMC at 77 K and from using exact Clapeyron equation applied to the experimental excess isotherms 77K as a function of coverage.**

Direct comparison of enthalpies determined from the isosteric method or from computational simulations is difficult, because of assumptions inherent to computational simulations and the assumptions on the data analysis for the experimental calorimetric data. To compare with other enthalpy determination methods across the whole range of uptake, each peak would have to be assigned to a specific hydrogen uptake, which even if using an appropriate model (such as the absolute function presented in Eq.2) would be highly sensitive to the pressures used. In addition, the experiments were done at room temperature, where hydrogen uptakes are very small and the uncertainty of the measurements is greater. In order to reduce uncertainties, the DSC was used to determine the zero-coverage enthalpy only. The first exothermic peak in Fig. 4A (at ~500 secs) was integrated using OriginLab, and a value for the zero-coverage enthalpy was calculated (details in Supporting Information). This calculated experimental value was compared with the enthalpies calculated with the Clapeyron equation, which were previously determined and from the GEMC simulations at 77 K (details in Supporting Information). In Fig. 4B, the enthalpies for the MIL-101(Cr) determined from the Clapeyron method at 77 K are shown, along with the zero-coverage enthalpy from the calorimetry and the enthalpies of adsorption obtained from GEMC simulations at 77 K. The enthalpies determined from the Clapeyron equation were previously calculated [27] by averaging the enthalpies across all temperatures to enable comparisons between the virial and Clausius-Clapeyron equation across all temperatures. As was the case for the hydrogen uptakes, the enthalpies of adsorption from simulations and from the Clapeyron equation are in good agreement, and both are in good agreement with the zero-coverage enthalpy



obtained for calorimetry, with values between 4.5 and 7.0 kJ mol<sup>-1</sup>. The lowest coverage point (at 0.5 wt%) calculated from the Clapeyron equation at 77 K is 9.94 kJ mol<sup>-1</sup>. This is within the range reported by Latroche et al. [24] (9.3 – 10.0 kJ mol<sup>-1</sup>), who reached these values using microcalorimetry at low coverages for hydrogen in MIL-101(Cr). The enthalpies then decrease with coverage and are close to 2.0 kJ mol<sup>-1</sup> at 6 wt.%. The accurate determination of the enthalpies of adsorption has important implications for thermal management in hydrogen storage systems. If these rely on adsorbent materials, 77 K is the most likely temperature of operation and a difference as small as 1.0 kJ mol<sup>-1</sup> in estimating these enthalpies could represent a difference of almost 1 MJ of heat released upon absorption when considering a 4 kg hydrogen storage system, which is why it is important to improve our understanding of the differences between these methods of estimation.

## Conclusions

Hydrogen adsorption in metal-organic framework MIL-101(Cr) was analysed with a combination of methods that include variable pressure and temperature *in-situ* synchrotron powder X-ray diffraction and inelastic neutron scattering, modelling applied to excess experimental isotherms, molecular simulations and differential scanning calorimetry. The *in-situ* synchrotron X-ray diffraction shows negligible change in the unit cell of the MIL-101(Cr) at temperatures ranging from 80 to 300 K and at pressures up to 10 MPa, unlike other metal-organic frameworks from the MIL family, such as the MIL-53(Al), which under the same conditions shows pressure and temperature variance. This is important as the main assumptions in simulations and in the modelling of the experimental isotherms are the constant volume of adsorption. The simulation results show very good correlation with the absolute uptakes calculated from adsorption experiments at 77 K and provide an insight into the densification mechanism that happens at the molecular level. The simulations indicate that H<sub>2</sub> adsorption at a low pressure is mainly located in the super-tetrahedron (0.7 nm) and then with increasing pressure in the small (2.9 nm) and large (3.4 nm) cages. To further investigate this, inelastic neutron scattering was done at increasing hydrogen pressures, showing no signs of higher density (solid or liquid-like) adsorbed hydrogen. Modelling on the experimental excess isotherms indicates an adsorbed density around 72.4 kg m<sup>-3</sup>, which is smaller than the density of solid hydrogen density at 4 K and 1.2 MPa, which is 87.6 kg m<sup>-3</sup>. The results indicate that the smaller pores in MIL-101(Cr), which are 0.7 nm, are not small enough for high adsorbed densities, such as the solid-like densities seen in activated carbons. Finally, the enthalpies of adsorption are studied with a combination of the Clapeyron equation

**Final version, post review and revision.** Bimbo, N.; Aggarwal, H.; Zhang, K.; Mays, T. J.; Jiang, J.; Barbour, L. J.; Ting, V. P., Hydrogen adsorption in metal-organic framework MIL-101(Cr) - Adsorbate densities and enthalpies from sorption, neutron scattering, *in situ* X-ray diffraction, calorimetry, and molecular simulations. *ACS Applied Energy Materials* **2021**, *4*, 7839-7847. DOI: [10.1021/acsaem.1c01196](https://doi.org/10.1021/acsaem.1c01196).

applied to the experimental excess isotherms, simulations at 77 K, and differential scanning calorimetry done at room temperature, showing good correspondence, with zero-coverage values in the 4.5 – 6.0 kJ mol<sup>-1</sup> range and values of 2.0 kJ mol<sup>-1</sup> at 6 wt.% for the simulations and the Clapeyron method.

## Acknowledgements

The authors would like to thank the Engineering and Physical Sciences Research Council (EPSRC) for a Fellowship (EP/R01660X/1) and for Hydrogen and Fuel Cells SUPERGEN Hub projects (EP/E040071/1, EP/K021109/1, EP/L018365/1 and EP/J016454/1), STFC for the allocation of ISIS beamtime (Proposal number RB1320122), ESRF for allocation of time for *in-situ* X-ray diffraction on ID31 (MA-1761), and the University of Bath for International Mobility Funding to visit Stellenbosch University.

## Supporting Information

X-ray diffraction patterns for MIL-53(Al). Description of molecular simulations. Simulation snapshots of hydrogen adsorption in MIL-101(Cr). Description of inelastic neutron scattering experiments. Description of Differential Scanning Calorimetry experiments. Molecular simulation videos for H<sub>2</sub> adsorption in the small and large cage of MIL-101 at 10,000 kPa.

## References

1. Schlappbach, L. and A. Zuttel, *Hydrogen-storage materials for mobile applications*. *Nature*, 2001. **414**(6861): p. 353-358.
2. van den Berg, A.W.C. and C.O. Areal, *Materials for hydrogen storage: current research trends and perspectives*. *Chem. Commun.*, 2008(6): p. 668-681.
3. Thomas, K.M., *Hydrogen adsorption and storage on porous materials*. *Catal. Today*, 2007. **120**(3-4): p. 389-398.
4. Ahmed, A., S. Seth, J. Purewal, A.G. Wong-Foy, M. Veenstra, A.J. Matzger, and D.J. Siegel, *Exceptional hydrogen storage achieved by screening nearly half a million metal-organic frameworks*. *Nat. Commun.*, 2019. **10**(1): p. 1568.
5. Chen, Z., P. Li, R. Anderson, X. Wang, X. Zhang, L. Robison, L.R. Redfern, S. Moribe, T. Islamoglu, D.A. Gómez-Gualdrón, T. Yildirim, J.F. Stoddart, and O.K. Farha, *Balancing volumetric and gravimetric uptake in highly porous materials for clean energy*. *Science*, 2020. **368**(6488): p. 297-303.
6. United States Department of Energy. *Targets for Onboard Hydrogen Storage Systems for Light-Duty Vehicles*. Available from: [http://www1.eere.energy.gov/hydrogenandfuelcells/storage/pdfs/targets\\_onboard\\_hydro\\_storage.pdf](http://www1.eere.energy.gov/hydrogenandfuelcells/storage/pdfs/targets_onboard_hydro_storage.pdf) (Accessed March 2021).
7. Hirscher, M., V.A. Yartys, M. Baricco, J. Bellosta von Colbe, D. Blanchard, R.C. Bowman, D.P. Broom, C.E. Buckley, F. Chang, P. Chen, Y.W. Cho, J.-C. Crivello, F. Cuevas, W.I.F. David, P.E. de Jongh, R.V. Denys, M. Dornheim, M. Felderhoff, Y. Filinchuk, G.E.

- Froudakis, D.M. Grant, E.M. Gray, B.C. Hauback, T. He, T.D. Humphries, T.R. Jensen, S. Kim, Y. Kojima, M. Latroche, H.-W. Li, M.V. Lototskyy, J.W. Makepeace, K.T. Møller, L. Naheed, P. Ngene, D. Noréus, M.M. Nygård, S.-i. Orimo, M. Paskevicius, L. Pasquini, D.B. Ravnsbæk, M. Veronica Sofianos, T.J. Udovic, T. Vegge, G.S. Walker, C.J. Webb, C. Weidenthaler, and C. Zlotea, *Materials for hydrogen-based energy storage – past, recent progress and future outlook*. *J. Alloys Compd.*, 2020. **827**: p. 153548.
8. Poirier, E., R. Chahine, and T.K. Bose, *Hydrogen adsorption in carbon nanostructures*. *Int. J. Hydrogen Energy*, 2001. **26**(8): p. 831-835.
  9. Noguera-Diaz, A., N. Bimbo, L.T. Holyfield, I.Y. Ahmet, V.P. Ting, and T.J. Mays, *Structure-property relationships in metal-organic frameworks for hydrogen storage*. *Colloids Surf., A*, 2016. **496**: p. 77-85.
  10. Gogotsi, Y., R.K. Dash, G. Yushin, T. Yildirim, G. Laudisio, and J.E. Fischer, *Tailoring of Nanoscale Porosity in Carbide-Derived Carbons for Hydrogen Storage*. *J. Am. Chem. Soc.*, 2005. **127**(46): p. 16006-16007.
  11. Laudisio, G., R.K. Dash, J.P. Singer, G. Yushin, Y. Gogotsi, and J.E. Fischer, *Carbide-derived carbons: A comparative study of porosity based on small-angle scattering and adsorption isotherms*. *Langmuir*, 2006. **22**(21): p. 8945-8950.
  12. Sevilla, M., R. Mokaya, and A.B. Fuertes, *Ultrahigh surface area polypyrrole-based carbons with superior performance for hydrogen storage*. *Energy Environ. Sci.*, 2011. **4**(8): p. 2930-2936.
  13. Yushin, G., R. Dash, J. Jagiello, J.E. Fischer, and Y. Gogotsi, *Carbide-derived carbons: Effect of pore size on hydrogen uptake and heat of adsorption*. *Adv. Funct. Mater.*, 2006. **16**(17): p. 2288-2293.
  14. Ting, V.P., A.J. Ramirez-Cuesta, N. Bimbo, J.E. Sharpe, A. Noguera-Diaz, V. Presser, S. Rudic, and T.J. Mays, *Direct Evidence for Solid-like Hydrogen in a Nanoporous Carbon Hydrogen Storage Material at Supercritical Temperatures*. *ACS Nano*, 2015. **9**(8): p. 8249-8254.
  15. Silvera, I.F., *The Solid Molecular Hydrogens in the Condensed Phase - Fundamentals and Static Properties*. *Rev. Mod. Phys.*, 1980. **52**(2): p. 393-452.
  16. Tian, M., M.J. Lennox, A.J. O'Malley, A.J. Porter, B. Krüner, S. Rudic, T.J. Mays, T. Duren, V. Presser, L.R. Terry, S. Rols, Y.N. Fang, Z.L. Dong, S. Rochat, and V.P. Ting, *Effect of pore geometry on ultra-densified hydrogen in microporous carbons*. *Carbon*, 2021. **173**: p. 968-979.
  17. Broom, D.P., *Hydrogen storage materials : the characterisation of their storage properties*. 2011, London: Springer.
  18. Leu, F.C. and T.H. Chang, *A convenient TPD method for calculating the integral heat of sorption*. *J. Chin. Inst. Chem. Eng.*, 2002. **33**(3): p. 321-324.
  19. Lynch, J.F. and T.B. Flanagan, *Calorimetric Determination of Differential Heats of Absorption of Hydrogen by Palladium*. *J. Chem. Soc., Faraday Trans. 1*, 1974. **70**(5): p. 814-824.
  20. Matsumoto, A., K. Yamamoto, and T. Miyata, *Microcalorimetric Characterization of Hydrogen Adsorption on Nanoporous Carbon Materials*. *Characterization of Porous Solids VII - Proceedings of the 7th International Symposium on the Characterization of Porous Solids (Cops-VII)*, Aix-En-Provence, France, 26-28 May 2005, 2006. **160**: p. 121-128.
  21. Czepirski, L. and J. Jagiello, *Virial-Type Thermal Equation of Gas Solid Adsorption*. *Chem. Eng. Sci.*, 1989. **44**(4): p. 797-801.
  22. Rouquerol, F., J. Rouquerol, and K.S.W. Sing, *Adsorption by powders and porous solids : principles, methodology, and applications*. 1999, San Diego: Academic Press. xvi, 467 p.

23. Duren, T., Y.S. Bae, and R.Q. Snurr, *Using molecular simulation to characterise metal-organic frameworks for adsorption applications*. *Chem. Soc. Rev.*, 2009. **38**(5): p. 1237-1247.
24. Latroche, M., S. Surble, C. Serre, C. Mellot-Draznieks, P.L. Llewellyn, J.H. Lee, J.S. Chang, S.H. Jung, and G. Ferey, *Hydrogen storage in the giant-pore metal-organic frameworks MIL-100 and MIL-101*. *Angew. Chem., Int. Ed.*, 2006. **45**(48): p. 8227-8231.
25. Llewellyn, P.L., S. Bourrelly, C. Serre, A. Vimont, M. Daturi, L. Hamon, G. De Weireld, J.S. Chang, D.Y. Hong, Y.K. Hwang, S.H. Jung, and G. Ferey, *High uptakes of CO<sub>2</sub> and CH<sub>4</sub> in mesoporous metal-organic frameworks MIL-100 and MIL-101*. *Langmuir*, 2008. **24**(14): p. 7245-7250.
26. Streppel, B. and M. Hirscher, *BET specific surface area and pore structure of MOFs determined by hydrogen adsorption at 20 K*. *Phys. Chem. Chem. Phys.*, 2011. **13**(8): p. 3220-3222.
27. Bimbo, N., J.E. Sharpe, V.P. Ting, A. Noguera-Diaz, and T.J. Mays, *Isosteric enthalpies for hydrogen adsorbed on nanoporous materials at high pressures*. *Adsorption*, 2014. **20**(2-3): p. 373-384.
28. Bimbo, N., W. Xu, J.E. Sharpe, V.P. Ting, and T.J. Mays, *High-pressure adsorptive storage of hydrogen in MIL-101 (Cr) and AX-21 for mobile applications: Cryocharging and cryokinetics (vol 89, pg 1086, 2016)*. *Mater. Des.*, 2016. **91**: p. 440-440.
29. Sharpe, J.E., N. Bimbo, V.P. Ting, A.D. Burrows, D.M. Jiang, and T.J. Mays, *Supercritical hydrogen adsorption in nanostructured solids with hydrogen density variation in pores*. *Adsorption*, 2013. **19**(2-4): p. 643-652.
30. Schneemann, A., V. Bon, I. Schwedler, I. Senkovska, S. Kaskel, and R.A. Fischer, *Flexible metal-organic frameworks*. *Chem. Soc. Rev.*, 2014. **43**(16): p. 6062-6096.
31. Coudert, F.-X., *Responsive Metal–Organic Frameworks and Framework Materials: Under Pressure, Taking the Heat, in the Spotlight, with Friends*. *Chem. Mater.*, 2015. **27**(6): p. 1905-1916.
32. Loiseau, T., C. Serre, C. Huguenard, G. Fink, F. Taulelle, M. Henry, T. Bataille, and G. Ferey, *A rationale for the large breathing of the porous aluminum terephthalate (MIL-53) upon hydration*. *Chem. – Eur. J.*, 2004. **10**(6): p. 1373-1382.
33. Yu, Z.W., J. Deschamps, L. Hamon, P.K. Prabhakaran, and P. Pre, *Modeling hydrogen diffusion in hybrid activated carbon-MIL-101(Cr) considering temperature variations and surface loading changes*. *Microporous Mesoporous Mater.*, 2017. **248**: p. 72-83.
34. Rallapalli, P.B.S., M.C. Raj, S. Senthilkumar, R.S. Somani, and H.C. Bajaj, *HF-free synthesis of MIL-101(Cr) and its hydrogen adsorption studies*. *Environ. Prog. Sustainable Energy*, 2016. **35**(2): p. 461-468.
35. Jiang, J.W. and S.I. Sandler, *Monte Carlo simulation of O<sub>2</sub> and N<sub>2</sub> mixture adsorption in nanoporous carbon (C-168 Schwarzite)*. *Langmuir*, 2003. **19**(14): p. 5936-5941.
36. Bimbo, N., V.P. Ting, A. Hruzewicz-Kolodziejczyk, and T.J. Mays, *Analysis of hydrogen storage in nanoporous materials for low carbon energy applications*. *Faraday Discuss.*, 2011. **151**: p. 59-74.
37. Toth, J., *State equations of solid-gas interface layers*. *Acta Chim. Acad. Sci. Hung.*, 1971. **69**(3).
38. Toth, J., *Gas-(dampf-) adsorption an festen oberflächen inhomogener aktivitat .1*. *Acta Chim. Acad. Sci. Hung.*, 1962. **30**(4).
39. Leachman, J.W., R.T. Jacobsen, S.G. Penoncello, and E.W. Lemmon, *Fundamental Equations of State for Parahydrogen, Normal Hydrogen, and Orthohydrogen*. *J. Phys. Chem. Ref. Data*, 2009. **38**(3).

**Final version, post review and revision.** Bimbo, N.; Aggarwal, H.; Zhang, K.; Mays, T. J.; Jiang, J.; Barbour, L. J.; Ting, V. P., Hydrogen adsorption in metal-organic framework MIL-101(Cr) - Adsorbate densities and enthalpies from sorption, neutron scattering, *in situ* X-ray diffraction, calorimetry, and molecular simulations. *ACS Applied Energy Materials* **2021**, *4*, 7839-7847. DOI: [10.1021/acsaem.1c01196](https://doi.org/10.1021/acsaem.1c01196).

40. Colognesi, D., M. Celli, A.J. Ramirez-Cuesta, and M. Zoppi, *Lattice vibrations of para-hydrogen impurities in a solid deuterium matrix: An inelastic neutron scattering study*. *Phys. Rev. B*, 2007. **76**(17), 174304.
41. Ramirez-Cuesta, A.J., M.O. Jones, and W.I.F. David, *Neutron scattering and hydrogen storage*. *Mater. Today*, 2009. **12**(11): p. 54-61.
42. Hruzewicz-Kolodziejczyk, A., V.P. Ting, N. Bimbo, and T.J. Mays, *Improving comparability of hydrogen storage capacities of nanoporous materials*. *Int. J. Hydrogen Energy*, 2012. **37**(3): p. 2728-2736.
43. Rzepka, M., P. Lamp, and M.A. de la Casa-Lillo, *Physisorption of hydrogen on microporous carbon and carbon nanotubes*. *J. Phys. Chem. B*, 1998. **102**(52): p. 10894-10898.

## Table of Contents graphic

